

INVESTIGATION OF DYNAMICALLY LOADED STRUCTURES USING THE FINITE ELEMENT METHOD

ÁDÁM KOWÁCS

Technical University of Budapest

The paper presents an application of the so-called implicit-explicit finite element method to the solution of geometrically and materially non-linear dynamic problems. The method has been implemented in IBM PC and its main features are shown through three simple examples.

1. Introduction

Dynamic loads can be caused due to high velocity metalworking (e.g. forging) in industrial circumstances or to impact, explosions and earthquakes which are of considering importance in the safety studies of nuclear reactors in hypothetical accidents, automotive and air-craft phenomena, and many other areas.

In the former case because of the finite strains occurred the correct mechanical analysis is rather difficult, while in the latter case numerous methods have been presented, which assume small strains, but allow large displacements as well as material nonlinearity.

In most of the numerical solutions of dynamic problems the equations of motion are first discretised in space. The discretisation using finite elements yields a set of ordinary differential equations in time. There are two basic types of methods for integrating the equations of motion: direct integration methods and modal superposition techniques. The modal superposition technique is normally used for linear problems only. The direct integration methods can be further subdivided into explicit and implicit methods. In explicit methods difference equations are used that permit the displacements at the next time step to be found in terms of the accelerations and displacements at the previous time step, so that the procedure does not involve the solution of any equations. In implicit methods the difference equations for the displacements at the next time step involve the accelerations at the next time step, so the determination of the displacements involves the solution of a system of equations.

For this reasons implicit algorithms usually require considerably more computational effort per time step as compared with explicit methods. On the other hand, explicit algorithms require very small time steps to ensure numerical stability, while in implicit methods the time step is only restricted by accuracy requirements.

To circumvent these difficulties, methods have been developed in which it is attempted to simultaneously achieve the attributes of both algorithms. For linear systems Hughes and Liu [1, 2] introduced the implicit-explicit concept. In their method the elements are partitioned into implicit and explicit sets. This concept was extended to non-linear problems by Hughes et al. [3]. Based on this method a finite element program has been published in [4]. This program dealt with plane stress, plane strain and axisymmetric applications.

Geometrically and materially non-linear behaviour was taken into account using a total Lagrangian formulation and a linear elastic-plastic isotropic hardening model. Isotropic hardening model does not include Bauschinger-effect which was experimentally observed during cycling loadings. The alternation of loadings and unloadings in the dynamic problems is similar to cycling loading, so that a kinematic hardening rule probably give a more accurate solution. Szabó and Kovács [5] publicate a subroutine which is based upon the exact integration of Prager's kinematic hardening rule presented by Xucheng and Liangming [6].

In the following the application of the modified version of the program mentioned, adapted to IBM PC will be shown.

2. Finite element formulation

After the spatial discretisation the resulting system of equations of motion for the dynamic problem becomes at time step $t_n + \Delta t$:

$$\mathbf{M} \cdot \ddot{\mathbf{d}}_{n+1} + \mathbf{P}_{n+1}(\mathbf{d}) = \mathbf{F}_{n+1}(t), \quad (1)$$

in which \mathbf{d} is the nodal displacement vector, \mathbf{M} is the structural mass matrix, $\mathbf{F}_{n+1}(t)$ are the applied or activating forces, dots denote differentiation in time. The term \mathbf{P}_{n+1} is the internal set of forces.

In non-linear cases \mathbf{P}_{n+1} can be estimated as:

$$\begin{aligned} \mathbf{P}_{n+1} &= \mathbf{P}_n + \mathbf{K}_n \cdot \Delta \mathbf{d}, \\ \Delta \mathbf{d} &= \mathbf{d}_{n+1} - \mathbf{d}_n, \end{aligned} \quad (2)$$

where \mathbf{K}_n is the tangential stiffness matrix evaluated from conditions at time t_n . \mathbf{K}_n can be divided into two parts:

$$\mathbf{K}_n = \mathbf{K}_L + \mathbf{K}_{NL}. \quad (3)$$

The linear stiffness matrix can be calculated as:

$$\mathbf{K}_L = \int_V \mathbf{B}^T \mathbf{D}^{ep} \mathbf{B} dV, \quad (4)$$

where \mathbf{B} is the strain-displacement matrix, \mathbf{D}^{ep} is the constitutive matrix.

The non-linear stiffness matrix is given as ([4]):

$$\mathbf{K}_{NL} = \int_V \mathbf{G}^T \cdot \mathbf{H} \cdot \mathbf{G} dV, \quad (5)$$

in which \mathbf{H} is a stress matrix formed from the components of the σ_n . Piola-Kirchhoff stresses, and \mathbf{G} is a matrix, which includes the derivatives of the shape functions.

3. Material nonlinearity

Prager's kinematic hardening rule can be written as:

$$\dot{S} = 2G \cdot \dot{\epsilon}' - \frac{9G^2}{\sigma_F^2(3G+H')} \mathbf{a} \cdot \mathbf{a}^T \cdot \dot{\epsilon}', \quad (6)$$

$$\mathbf{a} = S - \alpha,$$

where S is the vector of the stress deviatoric tensor, α is the vector of the translation tensor of the coordinates of the center of the yield surface, ϵ' is the vector of the strain deviatoric tensor, G is the shear modulus of the material, σ_F is the yield stress. The following relation can be written for α and for the plastic strain rate:

$$\dot{\alpha} = \frac{2}{3} H' \cdot \dot{\epsilon}^P = \frac{2GH' \cdot \mathbf{a}^T \cdot \dot{\epsilon}'}{R_0^2(3G+H')} \mathbf{a}, \quad (7)$$

where $R_0 = \sqrt{\frac{2}{3}} \sigma_F$ denotes the radius of the yield surface in the stress deviatoric space (Fig. 1).

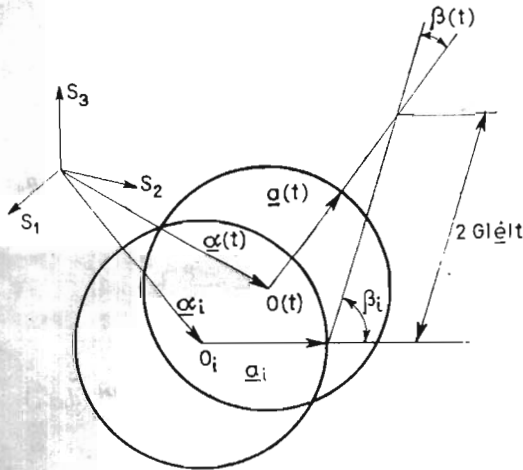


Fig. 1. Yield surfaces in the stress deviatoric space

From eqs. (6) and (7) after some transformation and integration detailed in [5] and [6] finally we obtain:

$$\alpha_{i+1} = \alpha_i + l \cdot [(1-p) \cdot a_i + 2 \cdot b \cdot G \cdot \Delta \epsilon'], \quad (8)$$

$$a_{i+1} = p \cdot a_i + 2 \cdot q \cdot G \cdot \Delta \epsilon', \quad (9)$$

where b , l , p , and q are constants depending on β_i , R_0 , and Δt , G is the shear modulus, and $\Delta \epsilon' = \dot{\epsilon}' \cdot \Delta t$.

Using eqs. (8) and (9), from the known σ_i , α_i quantities at time t_i with the strain increment $\Delta \epsilon$, we can obtain the unknown σ_{i+1} , α_{i+1} quantities as follows:

$$S_{i+1} = a_{i+1} + \alpha_{i+1}, \quad (10)$$

$$\sigma_{t+1} = S_{t+1} + K \cdot (\dot{\mathbf{i}}^T \cdot \Delta \varepsilon) \cdot \mathbf{i} + \frac{1}{3} (\dot{\mathbf{i}}^T \cdot \sigma_t) \cdot \mathbf{i}, \quad (11)$$

where:

$$K = E/[3(1-2\nu)] \text{ and } \dot{\mathbf{i}}^T = [1 \ 1 \ 0 \ 1],$$

E is the Young-modulus, ν is the Poisson ratio.

4. Implicit-explicit algorithm

In the implicit-explicit method the finite element mesh contains two groups of elements: the implicit group and the explicit group. The superscripts I and E will henceforth refer to the implicit and explicit groups, respectively.

In the implicit-explicit algorithm we iterate within each time step in order to satisfy the equation of motion:

$$\mathbf{M} \cdot \ddot{\mathbf{d}}_{n+1} \mathbf{P}^I + (\mathbf{d}_{n+1}) + \mathbf{P}^E(\mathbf{d}_{n+1}) = \mathbf{F}_{n+1}, \quad (12)$$

in which $\mathbf{M} = \mathbf{M}^I + \mathbf{M}^E$, $\mathbf{F}_{n+1} = \mathbf{F}_{n+1}^I + \mathbf{F}_{n+1}^E$ and $\tilde{\mathbf{d}}_{n+1} = \mathbf{d}_{n+1}^{[0]}$.

We assume that \mathbf{M}^E is diagonal.

The algorithm is as follows ([4]):

1. step — Set iteration counter: $i = 0$.
2. step — Begin predictor phase in which we set:

$$\mathbf{d}_{n+1}^{[i]} = \tilde{\mathbf{d}}_{n+1} = \mathbf{d}_n + \Delta t \cdot \dot{\mathbf{d}}_n + \frac{\Delta t^2}{2} (1-2\beta) \cdot \ddot{\mathbf{d}}_n,$$

$$\dot{\mathbf{d}}_{n+1}^{[i]} = \dot{\mathbf{d}}_n + \Delta t \cdot (1-\gamma) \cdot \ddot{\mathbf{d}}_n,$$

$$\ddot{\mathbf{d}}_{n+1}^{[i]} = \mathbf{0}.$$

3. step — Evaluate residual forces using the equation:

$$\Psi^{[i]} = \mathbf{F}_{n+1} - \mathbf{M} \cdot \ddot{\mathbf{d}}_{n+1}^{[i]} - \mathbf{P}^I(\mathbf{d}_{n+1}^{[i]}) - \mathbf{P}^E(\tilde{\mathbf{d}}_{n+1}).$$

4. step — If required, form the effective stiffness matrix:

$$\mathbf{K}^* = \frac{1}{\Delta t^2 \cdot \beta} \mathbf{M} + \mathbf{K}_n^I.$$

Otherwise use a previously calculated \mathbf{K}^* .

5. step — Solve the following system of linear equations:

$$\mathbf{K}^* \cdot \Delta \mathbf{d}_{n+1}^{[i]} = \Psi_{n+1}^{[i]}.$$

6. step — Enter corrector phase in which we set:

$$\mathbf{d}_{n+1}^{[i+1]} = \mathbf{d}_{n+1}^{[i]} + \Delta \mathbf{d}_{n+1}^{[i]},$$

$$\dot{\mathbf{d}}_{n+1}^{[i+1]} = \frac{1}{\Delta t^2 \beta} (\mathbf{d}_{n+1}^{[i+1]} - \mathbf{d}_{n+1}^{[i]}),$$

$$\ddot{\mathbf{d}}_{n+1}^{[i+1]} = \dot{\mathbf{d}}_{n+1}^{[i+1]} + \Delta t \cdot \gamma \cdot \ddot{\mathbf{d}}_{n+1}^{[i]}.$$

7. step — Check convergence:

$$\frac{\|\Delta \mathbf{d}_{n+1}^{[i]}\|}{\|\mathbf{d}_{n+1}^{[i+1]}\|} \stackrel{?}{<} \varepsilon \begin{cases} \text{yes : } \rightarrow \text{ 8. step} \\ \text{no : } i = i + 1 \rightarrow \text{ 3. step,} \end{cases}$$

8. step — Set:

$$\mathbf{d}_{n+1} = \mathbf{d}_{n+1}^{[i+1]},$$

$$\dot{\mathbf{d}}_{n+1} = \dot{\mathbf{d}}_{n+1}^{[i+1]},$$

$$\ddot{\mathbf{d}}_{n+1} = \ddot{\mathbf{d}}_{n+1}^{[i+1]},$$

for use in the next time step. Set $n = n + 1$, form \mathbf{P} and begin the next time step.

5. Stability analysis

The implicit-explicit algorithm include three free parameters: γ , β , and Δt . Their values govern the accuracy and stability of the algorithm. Hughes and Liu [1] and Key [7] have discussed the stability limits for this scheme.

Unconditional stability of the implicit group is achieved with:

$$\gamma \geq \frac{1}{2} \quad \text{and} \quad \beta = \frac{\left(\gamma + \frac{1}{2}\right)^2}{4}. \quad (13)$$

The time step is then restricted by the explicit element group. The maximum stable time step is determined from:

$$\Delta t_{crit} \leq \frac{2}{\omega_{max}}, \quad (14)$$

where ω_{max} is the maximum frequency of the explicit group. We can estimate ω_{max} as:

$$\omega_{max} \leq \max_{(e)}(\omega_{max}^{(e)}), \quad (15)$$

where $\omega_{max}^{(e)}$ is the maximum frequency of the e -th element of the explicit group. If only implicit elements are used and the (13) conditions are satisfied, then for reasonable accuracy the time step should be limited to ([8]):

$$\Delta t < 0.01 T_{max}, \quad (16)$$

where T_{max} is the largest period. We can obtain T_{max} and ω_{max} from the solution of the generalised eigenvalue-eigenvector problem:

$$\mathbf{K} \cdot \Phi = \omega^2 \cdot \mathbf{M} \cdot \Phi, \quad (17)$$

and the inverse problem:

$$\mathbf{M} \cdot \Phi = \frac{1}{\omega^2} \mathbf{K} \cdot \Phi \quad (18)$$

respectively. Using the Stodola-iteration (Rayleigh-quotient) method we can find the largest period from eq. (17) with:

$$T_{\max} = \frac{2\pi}{\omega_{\min}}, \tag{19}$$

and ω_{\max} from eq. (34) with:

$$\omega_{\max} = \left(\frac{1}{\omega}\right)_{\min}. \tag{20}$$

6. Implementation

6.1. Elastic large displacements of a cantilever [9, 10, 12]. The cantilever in Fig. 2. was analysed for a uniformly distributed load using five 8-node plane stress isoparametric

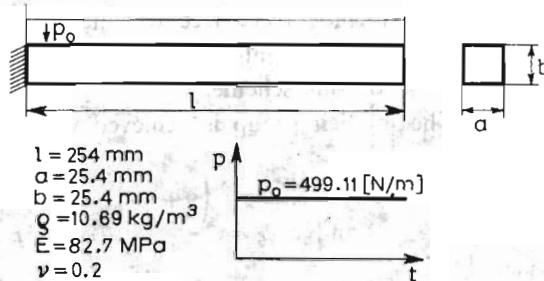


Fig. 2. Uniformly loaded cantilever

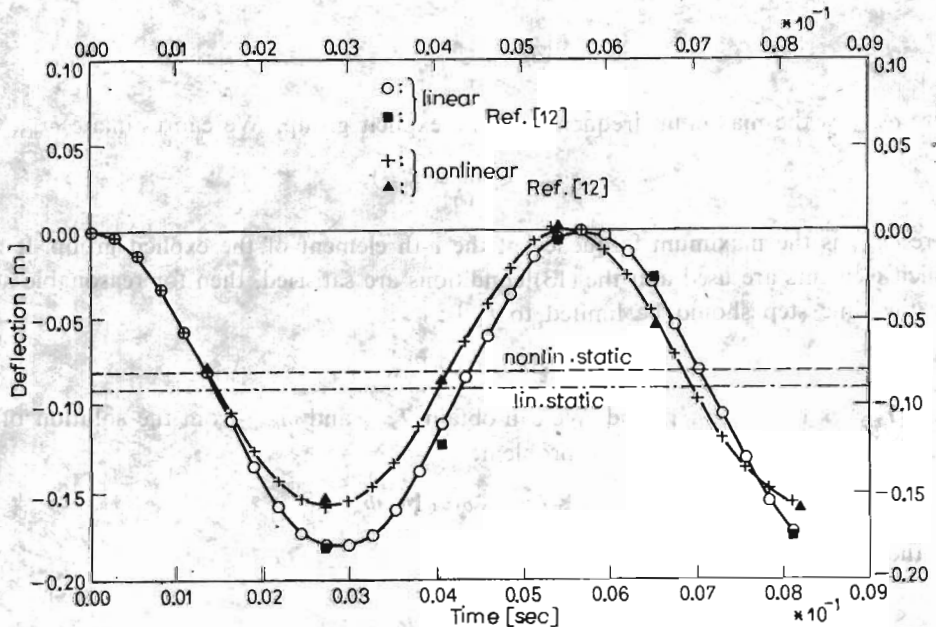


Fig. 3. Linear and non-linear transient response of the cantilever

elements. The materials of the cantilever was assumed to be isotropic and linear elastic. According to beam theory, the static small deflection is $w = 90.5$ [mm]. To calculate the large deflection we used the analytical solution given by Holden [11]. It was $w = 82.8$ [mm]. The linear transient response was determined by using the Laplace-transformation. Fig. 3. shows the comparison between linear and non-linear responses. The non-linear analysis was carried out using a time step $\Delta t \approx T_{max}/21 = 2.7 \cdot 10^{-4}$ [s]. The stiffening of the cantilever in the non-linear case markedly damps out the amplitude and shortens the period of oscillations.

6.2. Elasto-plastic dynamic response of a half-ring [14]. The half-ring shown in Fig. 4. was analysed with ten axisymmetric elements. Fig. 5. shows the vertical displacement at the

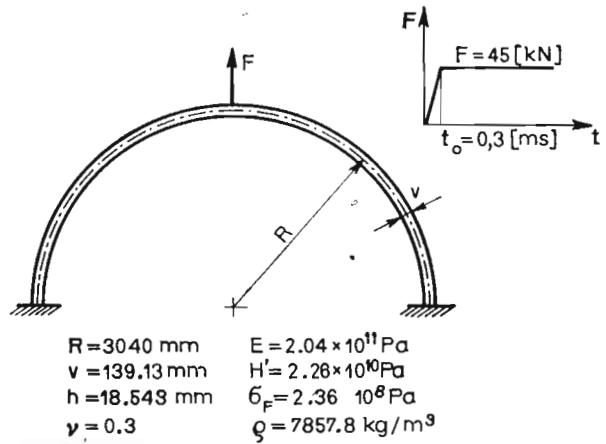


Fig. 4. Dynamically loaded half-ring

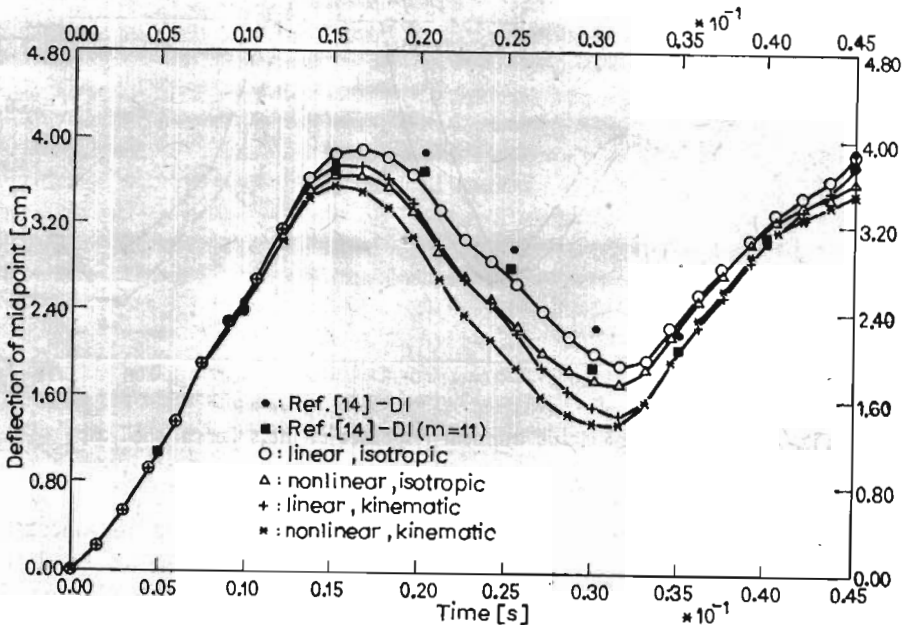


Fig. 5. Transient responses of the half-ring

midpoint given by isotropic and kinematic hardening model. The relatively good fit to the reference solutions in the isotropic case shows that isotropic hardening was probably used in [14]. The augmentation of the mean value of the oscillations is due to the plastic strains.

6.3. Elastic-plastic analysis of a spherical shell cap [4, 13, 15, 16]. Ten axisymmetric elements are used to make the finite element model of the spherical shell cap shown in Fig. 6. Fig. 7

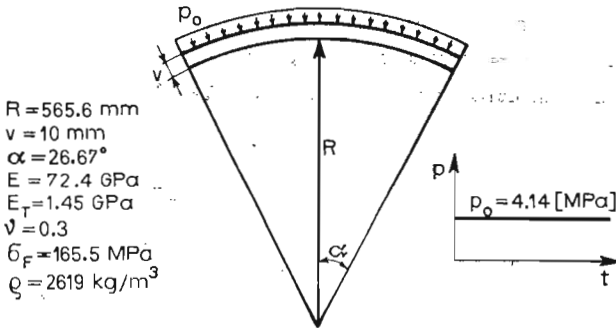


Fig. 6. Spherical shell cap submitted to step pressure loading

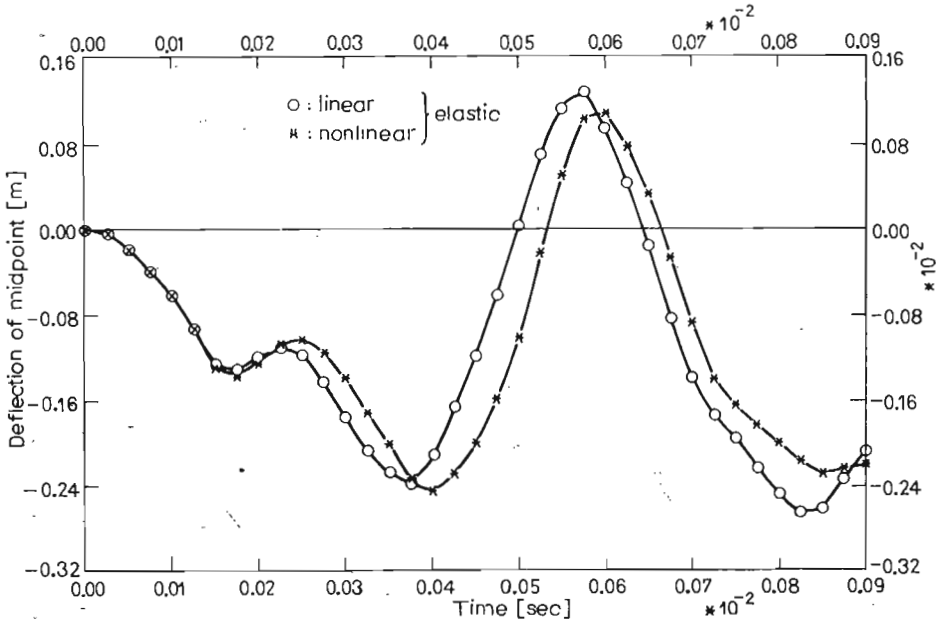


Fig. 7. Comparison of elastic transient responses of the spherical shell cap

and Fig. 8. shows the vertical displacement at mid point using materially linear and non-linear model. It is seen from the Figures that material and geometric non-linear effects are very significant. The amplitude decay and period elongation is due to the plastic deformation. In the reference solutions isotropic hardening was used. In linear analysis kinematic hardening does not modify the response as in the non-linear case.

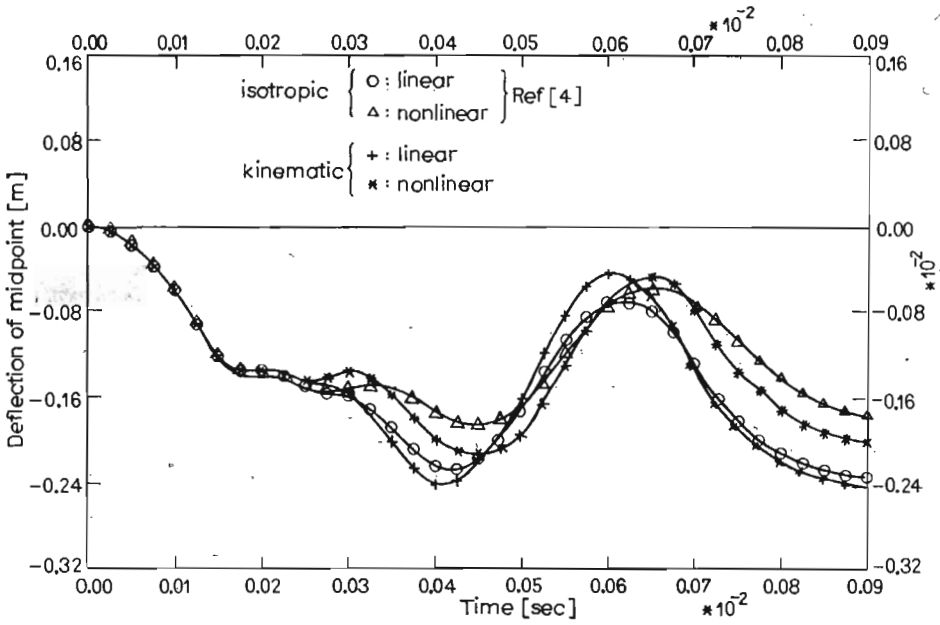


Fig. 8. Comparison of materially nonlinear transient responses of the spherical shell cap

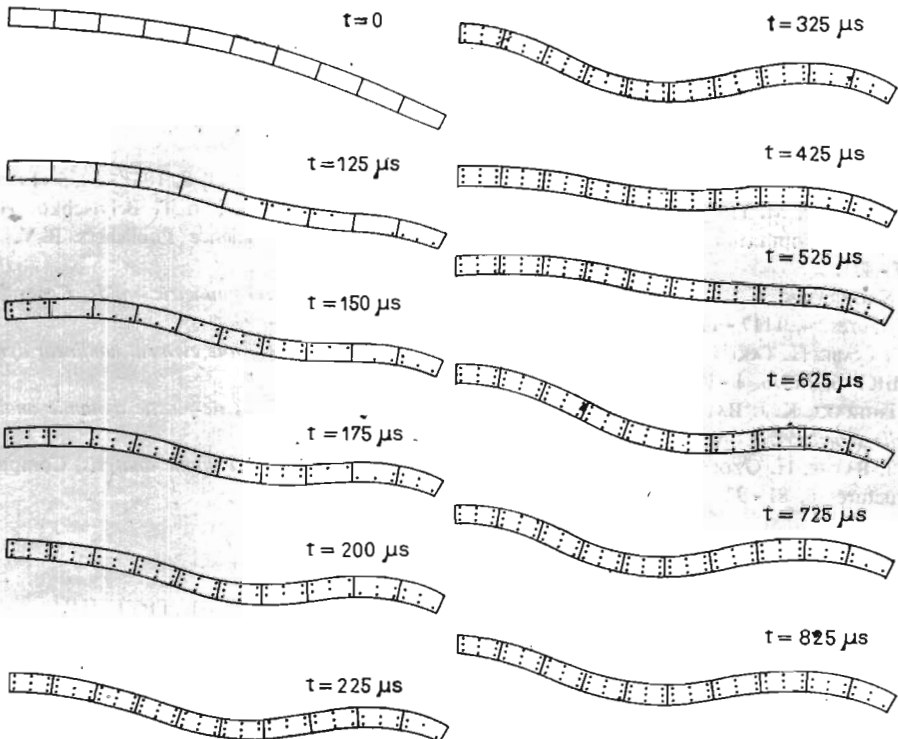


Fig. 9. Deformed shapes of the spherical shell cap with plastic zones

Assuming large displacements, with the use of kinematic hardening the deformed shapes with the instantaneous plastic zones in some moments are shown in Fig. 9.

An effective finite element method have been presented for calculating transient response of dynamically loaded structures. The so-called implicit-explicit algorithm is suitable to analyse geometrically and materially non-linear problems.

References

1. T. J. R. HUGHES, W. K. LIU, *Implicit-explicit finite elements in transient analysis: implementation and numerical examples*, J. Appl. Mech. ASME, 45, 375 - 378 (1978).
2. T. J. R. HUGHES, W. K. LIU, *Implicit-explicit finite elements in transient analysis: stability theory*, J. Appl. Mech. ASME, 45, 371 - 374 (1978).
3. T. J. R. HUGHES, K. S. PISTER, R. L. TAYLOR, *Implicit-explicit finite elements in nonlinear transient analysis*, Comp. Meth. Appl. Mech. Engng, 17/18, 159 - 182 (1979).
4. D. R. J. OWEN, E. HINTON, *Finite Elements in Plasticity. Theory and Practice*, Pineridge Press Ltd. Swansea U. K. (1980).
5. L. SZABÓ, Á KOVÁCS, *Numerical implementation of Prager's kinematic hardening model in exactly integrated form for elasto-plastic analysis*, Computers & Structures 26, 815 - 822 (1987).
6. W. XUCHENG, C. LIANGMING, *Exact integration of constitutive equations of kinematic hardening material nad its extended applications*, SMiRT 8, L2/3, 65 - 70 (1985).
7. S. W. KEY, *Transient response by time integration: review of implicit and explicit operators*, in J. Donéa: Advanced Structural Dynamics, Applied Science Publishers Ltd., London (1980) 71 - 95.
8. E. L. WILSON, I. FARHOOMAND, K. J. BATHE, *Nonlinear dynamic analysis of complex structures*, Earthquake Engineering and Structural Dynamics, 1, 241 - 252 (1973).
9. D. SHANTARAM, D. R. J. OWEN, O. C. ZIENKIEWICZ, *Dynamic transient behavior of two- and three-dimensional structures including plasticity, large deformation effects and fluid interaction*, Earthquake Engineering and Structural Dynamics, 4, 561 - 578 (1976).
10. K. J. BATHE, E. RAMM, E. L. WILSON, *Finite elements formulations for large deformation dynamic analysis*, Int. J. Num. Meth. Engng., 9, 353 - 386 (1975).
11. J. T. HOLDEN, *On the finite deflection of thin beams*, Int. J. Solids Struct, 8, 1051 - 1055 (1972).
12. M. GERADIN, M. HOGGE, S. IDELSSOHN, *Implicit finite element methods*, in T. Belytschko, Hughes, T. J. R.: Computational Methods for Transient Analysis, Elsevier Science Publishers B. V. (1983) 417 - 471.
13. S. NAGARAJAN, E. P. POPOV, *Elastic-plastic dynamic analysis of axisymmetric solids*, Computers & Structures, 4, 1117 - 1134 (1974).
14. M. TANABE, H. TAKEDA, *An efficient modal transformation method for finite element nonlinear dynamics*, SMiRT 6, M3/6, 1 - 9 (1981).
15. T. ISHIZAKI, K. J. BATHE, *On finite element large displacement and elastic-plastic dynamic analysis of shells structures*, Computers & Structures, 12, 309 - 318 (1980).
16. K. J. BATHE, H. OZDEMIR, *Elastic-plastic large deformation static and dynamic analysis*, Computers & Structures 6, 81 - 92 (1976).

Резюме

ИССЛЕДОВАНИЕ ДИНАМИЧЕСКИ НАГРУЖЕННЫХ КОНСТРУКЦИЙ МЕТОДОМ КОНЕЧНЫХ ЭЛЕМЕНТОВ

В работе применяем „явно-неявную” версию метода конечных элементов к решению геометрически и физически нелинейных динамических задач.

Вычисления сделано на „IBM PC” а главные черты метода были показаны на трёх несложных примерах.

Streszczenie

BADANIE DYNAMICZNIE OBCIĄŻONYCH KONSTRUKCJI METODĄ ELEMENTÓW
SKOŃCZONYCH

W pracy przedstawiono zastosowanie tak zwanej jawno-uwikłanej wersji metody elementów skończonych do rozwiązania geometrycznie i fizycznie nieliniowych zagadnień dynamicznych.

Obliczenia wykonano na IBM PC, a główne cechy metody pokazano na trzech prostych przykładach.

Praca wpłynęła do Redakcji dnia 10 grudnia 1987 roku.
